

## Dynamics of the constrained polymer collapse

I. S. ARANSON<sup>1</sup> and L. S. TSIMRING<sup>2</sup>

<sup>1</sup> *Materials Science Division, Argonne National Laboratory  
9700 S. Cass Avenue, Argonne, IL 60439, USA*

<sup>2</sup> *Institute for Nonlinear Science, University California, San Diego  
La Jolla, CA 92093-0402, USA*

(received 27 January 2003; accepted in final form 15 April 2003)

PACS. 61.25.Hq – Macromolecular and polymer solutions; polymer melts; swelling.

PACS. 83.10.Rs – Computer simulation of molecular and particle dynamics.

**Abstract.** – The dynamics of polymer collapse with a fixed distance between endpoints is studied analytically and numerically by the Nosé-Hoover algorithm. We find that at the pearling stage of the collapse the number of pearls decays as  $t^{-1/2}$  leading to anomalously long collapse time. To understand the effect of Stokes drag we reduced the problem of long-polymer-chain collapse to the one-dimensional diffusion-limited coalescence of particles with the mass-dependent mobility. In this case the number of pearls decays slower, as  $t^{-3/7}$ .

The conformational behaviour of long polymer chains under the action of hydrophobic forces is a topic of significant interest [1, 2]. At equilibrium the average size of an isolated polymer molecule depends strongly on the quality of the solvent, and varies from extended conformations in good solvents to collapsed states in poor solvents. The collapse is an integral part of the complex protein folding process. Recent experiments and numerical simulations revealed rich kinetics of the polymer collapse [3–11]. In particular, numerical studies indicate that the collapse of a polymer chain is mediated by the formation of numerous pearls (clusters of monomers) and subsequent coarsening of the pearls leading to the formation of a single large globule. When ends of a polymer chain are free, the coarsening of the pearled state occurs relatively fast [5]. The mechanism of coarsening is a mutual attraction of pearls due to the force exerted by pearls on the polymer chain connecting them.

The scaling properties and the kinetics of collapse are not completely understood. The problem becomes especially complex when the polymer is subject to various constraints, *e.g.* when it is submersed in a shear flow, its points are attached to walls or pulled externally. An interesting behaviour was observed when a biopolymer was stretched by the tip of an atomic-force microscope, see [12, 13]. Various non-trivial regimes in the polymers dynamics due to stretching by external force were studied in recent works [11, 14–18].

The kinetics of polymer chains with free ends studied in refs. [5, 7] yield a relatively short collapse time  $t_c \sim N^{1-1.5}$ , where  $N$  is the total number of monomers in the chain. Here we study the dynamics of the homopolymer collapse in case when the endpoints of the chain are fixed. Our numerical and analytical results show that the pearling stage of the homopolymer collapse of a chain with fixed endpoints proceeds much slower than for a free polymer. From

large-scale molecular-dynamics simulations using the Nosé-Hoover algorithm we find that the number of pearls  $N_p$  decays as  $t^{-1/2}$  leading to anomalously long collapse time  $t_c \sim N^2$ . This scaling is consistent with approximating the pearling stage of collapse as a diffusion-limited coalescence of pearls in one dimension with mass-independent diffusion. We verified in our numerical simulations that pearl mass and distance distribution functions are also close to those obtained from the one-dimensional diffusion-limited coalescence model with mass-independent diffusion. Hydrodynamic interaction between the polymer chain and the solvent of course would lead to the mass/size-dependent diffusion of pearls. Existing computing capabilities do not allow realistic modeling of the effects of the surrounding liquid on the long-polymer-chain motion. Anticipating that the surrounding solvent should mostly affect the mobility of pearls through the size-dependent Stokes drag, we estimated the expected scaling behaviour via a related one-dimensional problem of diffusion-limited coalescence of conglomerates with mass-dependent mobility. While this problem still cannot be solved exactly, we were able to derive scaling exponents and numerically find the cluster mass and inter-particle distance distribution functions. In this case the number of pearls decays even slower, as  $N_p \sim t^{-3/7}$ , and the collapse time is  $t_c \sim N^{7/3}$ .

*Molecular dynamics simulations* were performed using the Nosé-Hoover method permitting to work in the canonical ensemble (fixed temperature) [19]. Specific limitations related to the Nosé-Hoover algorithm will be discussed later. Monomers in a polymer chain of length  $N$  are connected by the strong anharmonic nearest-neighbor potential, and because of hydrophobic effects of the poor solvent interact with other monomers through long-range van der Waals forces. The Nosé-Hoover algorithm is expressed in terms of the following set of dynamic equations (see ref. [11] for details):

$$\dot{\mathbf{r}}_i = \mathbf{p}_i/m, \quad (1)$$

$$\dot{\mathbf{p}}_i = -\frac{\partial V_i}{\partial \mathbf{r}_i} - \xi \mathbf{p}_i, \quad (2)$$

$$\tau_\xi^2 \dot{\xi} = \frac{2K}{T} - (3N - 6), \quad (3)$$

where  $\mathbf{r}_i$ ,  $\mathbf{p}_i$  are positions and momenta of monomers,  $m$  is the monomer mass,  $\xi$  is the friction variable,  $T$  is the temperature (unit system with Boltzmann constant  $k_B = 1$  is assumed),  $\tau_\xi = 2Q/T$  is the time constant of the heat bath, and  $K = \sum p_i^2/2m$  is the kinetic energy. The potential  $V$  has two contributions,  $V = V_1(r) + V_2(r)$ , where  $V_1(r) = a(r - d_0)^2 + b(r - d_0)^4$  defines the valence interaction between neighboring monomers ( $r$  is the inter-atom distance,  $d_0$  is the equilibrium distance and  $a$ ,  $b$  are constants);  $V_2$  implements the Lennard-Jones attraction between non-neighboring monomers,  $V_2 = \epsilon[(\sigma/r)^{12} - (\sigma/r)^6]$  for  $r < r_0$  and  $V_2 = 0$  otherwise, where  $\sigma$  is the van der Waals radius and  $\epsilon$  is the potential depth,  $r_0$  is the cut-off radius. The parameters of our simulations are  $m = d_0 = \sigma = 1$ ,  $\epsilon = 1$ ,  $a = 30$ ,  $b = 100$ ,  $Q = 10$ ,  $r_0 = 6\sigma$ . For the chosen parameters the  $\Theta$ -point corresponds to  $T \approx 0.7$  [11]. The coupling constant with the thermostat  $Q$  was chosen to be close to optimal coupling  $Q_c \approx \sqrt{3NT}/4\omega$ , where  $\omega^2 \sim 2a$  is the typical frequency of monomer oscillation, see [20] for discussion. Simulations were performed for different values of  $Q = 5-15$ , and no significant difference was detected. This algorithm has been implemented on a massive parallel computer. Although it does not take into account the realistic hydrodynamic interaction between the polymer chain and the solvent, we believe that it yields qualitatively correct overall dynamics of collapse. The corrections due to hydrodynamic effects (in particular, Stokes drag) are discussed later.

We used long chains of up to  $N = 20000$  monomers, and the simulation time was as large as 5000 dimensionless units. Typically, four runs with different initial conditions were performed

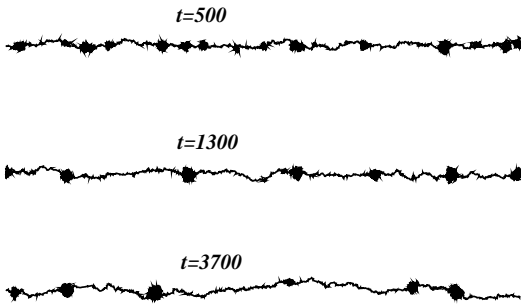


Fig. 1

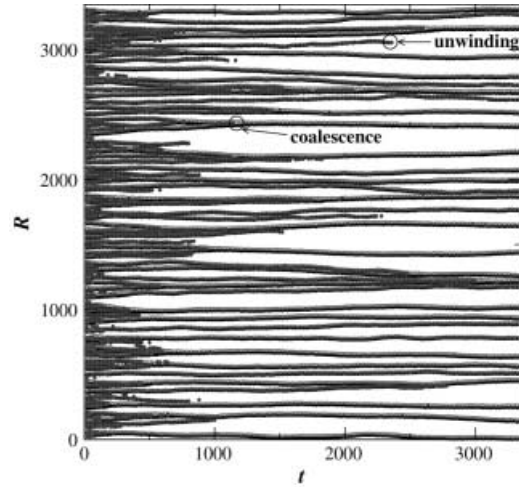


Fig. 2

Fig. 1 – Sequence of polymer configurations for three different moments of time, number of monomers  $N = 20000$ , temperature  $T = 0.4$ , approximately a quarter of the total chain is shown.

Fig. 2 – Space-time diagram illustrating the evolution of the polymer chain.  $R$  is the distance to the left endpoint, dots and circles indicate the leftmost and rightmost monomers in pearls; parameters as for fig. 1.

for each set of parameter values to obtain sufficient statistics. We varied temperature  $T$  and the chain length  $N$ . Initial configurations were prepared by creating a uniformly curved chain configuration (typically a helix or a circular arc) with fixed endpoint positions at the distance about 20–30% of the total length. The distance between end points  $L_0$  was selected from the condition  $N^{1/3} \ll L_0/d_0 < N$ , *i.e.* the polymer should not be too stretched and the endpoints should not be too close. We added small perturbations to the positions of the monomers, and abruptly quenched the temperature below the  $\Theta$ -point.

Immediately after the quench, pearls begin to form spontaneously, which leads to gradual straightening and tightening of the chain (time  $t \leq 100$ – $150$  dimensionless units). This initial tightening of the chain is obvious from fig. 3, inset (see below), showing the relative extension of the chain segments between the pearls,  $S = \sum_i L_i / \sum_i d_0 N_i$ , where  $L_i$  is the arclength of the chain segment between  $i$  and  $i + 1$  pearl, and  $N_i$  is the number of monomers in this segment. The force  $F$  acting on the endpoint of the chain is related to extension  $S$  as  $F \sim S - 1$ . After the chain becomes nearly straight, the tension approaches the quasi-equilibrium value, a much slower process of pearl coalescence begins. It is characterized by the drift and coalescence between pearls, whereas the chain segments between pearls remain practically straight, fig. 1. Eventually, it leads to the formation of one big globule.

The coalescence-dominated character of the polymer collapse is evident from the space-time diagram showing the positions of leftmost and rightmost monomers within pearls, fig. 2. As seen in the figure, pearls perform random walk along the chain (diffusion) and disappear mostly via coalescence after collision, and only a small fraction disappears through unwinding. In the process of diffusion the positions of the leftmost and rightmost monomers in the pearls remain strongly correlated due to the long-range van der Waals interaction which holds the pearls together. We calculated the diffusion constant of the pearl motion between collisions

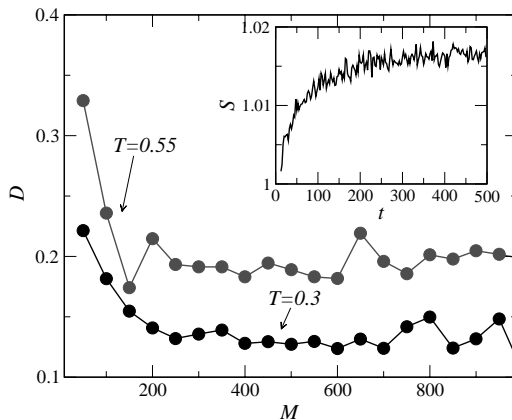


Fig. 3 – Pearl diffusion coefficient  $D$  vs. pearl mass  $M$  for two values of temperature. Inset: relative chain extension  $S$  vs.  $t$  for a chain of  $N = 8000$  monomers,  $T = 0.3$ .

and found that it is practically independent of pearl mass (fig. 3) except for the small mass range where the diffusion is enhanced.

The independence of the mobility from the pearl mass which leads to some underestimation of dissipation and the collapse time is an apparent artifact of the Nosé-Hoover method. This method does not take into account the size-dependent viscous drag force between pearls and the solvent according to the Stokes-Einstein relation [21]. Indeed, averaging the momentum equation (2) over one pearl, we obtain an equation for the pearl center of mass with size-independent friction coefficient  $\xi$  which weakly depends on time through the kinetic energy  $K$ . An alternative approach could consist in applying frictional Langevin dynamics or Monte Carlo method to individual monomers. However, in this case because of neglected screening effects within beads one can expect the friction constant to be proportional to the bead mass (Rouse scaling) which would lead to overestimation of dissipation and collapse time. We have chosen the Nosé-Hoover algorithm which is computationally more effective and appears to yield qualitatively correct behavior. One should realize, however, that the true value of the scaling exponent can be obtained only from simulations treating the solvent explicitly.

We studied the scaling properties of the number of pearls  $N_p$  vs. time and found that in a wide range of parameters the power law dependence holds  $N_p \sim t^{-s}$ , where the scaling exponent  $s \approx 0.5$  (see fig. 4), although for small temperatures some long transient occurs. This behaviour yields anomalously long collapse time  $t_c \sim N^{1/s} = N^2$ .

The scaling exponent  $s$  can be derived from the following argument. As we have found, in our simulations the pearls perform an ordinary random walk along the chain with the diffusion constant  $D$  almost independent of the pearl mass. Then it is easy to see that after time  $t$  all pearls within an interval  $l = \sqrt{Dt}$  coalesce into a single pearl, and so the average number of pearls at time  $t$  is

$$N_p = \frac{L_0}{l} \propto \frac{1}{\sqrt{Dt}}, \quad (4)$$

where  $L_0$  is the distance between the endpoints of the chain. This result is in agreement with MD simulations (see analytical lines in fig. 4).

The dynamic behaviour exhibited by a long polymer chain resembles the diffusion-limited coalescence (DLC) of particles in one dimension [22–24]. In this process the coalescence of two point particles with masses  $M_{1,2}$  results in a particle with mass  $M_1 + M_2$ . DLC with the mass-

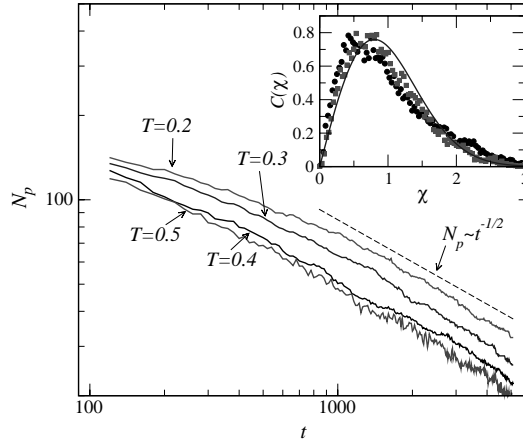


Fig. 4 – Number of pearls  $N_p$  vs. time in log-log scale for different values of temperature  $T$ . Inset: inter-particle distribution function  $C(l)$  vs.  $\langle l \rangle$  (circles) and cluster mass distribution function  $C(M)$  vs.  $M/\langle M \rangle$  (squares) for  $T = 0.3$ . The solid line shows the theoretical dependence  $C = \frac{\pi\chi}{2} \times \exp[-\pi\chi^2/4]$ .

independent mobility of particles can be solved exactly in one dimension [23,24]. It yields the same scaling  $N_p \sim 1/\sqrt{t}$ . DLC is characterized by two distribution functions: cluster mass distribution function  $C(M)$  (CMDF) and inter-particle distribution function  $C(L)$  (IPDF). Both functions have the same self-similar functional dependence in the asymptotic regime  $t \rightarrow \infty$ :  $C(\chi) \rightarrow \frac{\pi\chi}{2} \exp[-\pi\chi^2/4]$ , where  $\chi = M/\langle M \rangle$  or  $L/\langle L \rangle$  is the self-similar variable. We found both CMDF and IPDF from our simulations (fig. 4, inset). The distribution functions are averaged over 4 different sets of initial conditions and 250 moments of time. As follows from the figure, the results for both CMDF and IPDF agree with the theoretical dependence for 1D DLC with mass-independent diffusion.

Simulation of collapse of long polymer chains with realistic solvent effects is still far beyond reach of modern computers. Collapse of relatively short chains with simplified hydrodynamics was studied in refs. [8, 9]. These simulations with explicitly incorporated solvent indicate faster collapse than in the case when solvent is included only through van der Waals forces between the monomers. At least for short polymers with open ends, refs. [8, 9] found that hydrodynamic effects alter the collapse pathway, allowing folding to occur homogeneously along the chain, rather than initially at the chain ends. As was discussed above, the absence of hydrodynamic effects in the Nosé-Hoover approximation leads to the mass-independent mobility of pearls. Assuming that in real solvent the bead motion is controlled by the Stokes drag, the pearl diffusion constant can be estimated via the Stokes-Einstein relation

$$D \sim T/R \sim T/M^{1/3}, \quad (5)$$

where  $R \sim M^{1/3}$  is the pearl size [21]. Substituting eq. (5) into eq. (4) and taking into account that  $M = M_0/N_p$ , where  $M_0$  is the total mass, one obtains the corrected scaling law  $N_p \sim t^{-3/7}$ . Accordingly, the collapse time will scale as  $t_c \sim N^{7/3}$ , *i.e.* the effect of viscous drag modifies the scaling exponent obtained from the Nosé-Hoover algorithm by about 15%.

To obtain an additional insight into the effect of the Stokes drag on the polymer chain collapse, we performed Monte Carlo simulations of the one-dimensional diffusion-limited point particle coalescence with mass-dependent diffusion coefficient  $D = D_0 M^{-1/3}$ . We used up to 5000 particles in the system of length 20000. The simulations were performed using asyn-

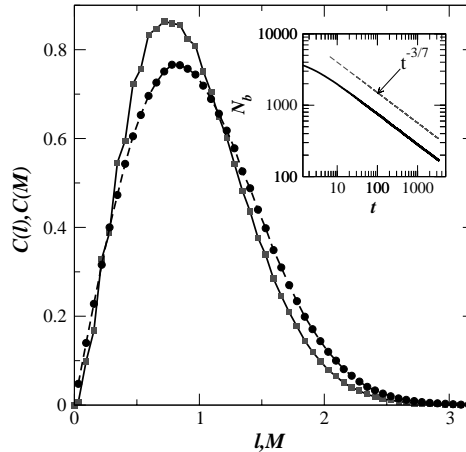


Fig. 5 – Main plot: CMDF (squares) and IPDF (circles) *vs.* self-similar variable  $\chi = M/\langle M \rangle, L/\langle L \rangle$  values for  $D_0 = 0.4$ . Inset: number of particles  $N_p$  *vs.* time; the dashed line shows the power law  $N_p \sim t^{-3/7}$ .

chronous update. Selected results are shown in fig. 5. The number of pearls decays as  $t^{-3/7}$  in agreement with our scaling argument. In contrast to the constant-diffusion case [22–24], CMDF and IPDF exhibit different asymptotic behaviours: the small-mass region of the CMDF is underpopulated comparing to that of the DLC with mass-independent mobility. It is a consequence of the mass-dependent mobility: light clusters have larger mobility and, therefore, have higher collision rate and disappear rapidly.

In conclusion, we studied the dynamics of homopolymer collapse in the regime when the distance between the endpoints is fixed. From the molecular-dynamics simulations neglecting the hydrodynamic effects (Nosé-Hoover approximation), we find that the pearling stage of the collapse satisfies a scaling relation with the number of pearls decaying as  $t^{-1/2}$ , but we expect the scaling exponents to change to  $-3/7$  when the Stokes drag is included. Fixing the endpoints of the chain is not the only type of constraints which can affect the dynamics of polymer collapse. One interesting unexplored possibility is the collapse of long polymer chains in shear flows and external fields. Another intriguing generalization of our analysis would be analysis of the collapse of a heteropolymer with controlled (*e.g.* periodic) heterogeneity.

\*\*\*

We thank T. FRISCH and A. GROSBURG for stimulating discussions, and D. VOLFOSON for help in simulations. This work was supported by the US DOE under grants W-31-109-ENG-38 and DE-FG03-95ER14516. Simulations were performed at the National Energy Research Scientific Computing Center.

## REFERENCES

- [1] DE GENNES P.-G., *Scaling Concepts in Polymer Physics* (Cornell University Press, Ithaca) 1988.
- [2] GROSBURG A. YU. and KHOKHLOV A. R., *Statistical Mechanics of Macromolecules* (AIP Press, New York) 1994.
- [3] WU C. and ZHOU S., *Phys. Rev. Lett.*, **77** (1996) 3053.

- [4] BYRNE A., KIERNAN P., GREEN D. and DAWSON K. A., *J. Chem. Phys.*, **102** (1995) 573.
- [5] KUZNETSOV YA. A., TIMOSHENKO E. G. and DAWSON K. A., *J. Chem. Phys.*, **103** (1995) 4807; **104** (1995) 3338.
- [6] KLUSHIN L. I., *J. Chem. Phys.*, **108** (1998) 7917.
- [7] OSTROVSKY B., CROOKS G., SMITH M. A. and BAR-YAM Y., *Parallel Comput.*, **27** (2001) 613.
- [8] CHANG R. and YETHIRAJ A., *J. Chem. Phys.*, **114** (2001) 7678.
- [9] KIKUCHI N., GENT A. and YEOMANS J. M., *Eur. Phys. J. E*, **9** (2002) 66.
- [10] ABRAMS C. F., LEE N.-K. and OBUKHOV S. P., *Europhys. Lett.*, **59** (2002) 391.
- [11] FRISCH T. and VERGA A., *Phys. Rev. E*, **65** (2002) 041801; **66** (2002) 041807.
- [12] OBERHAUSER A. F. *et al.*, *Nature (London)*, **393** (1998) 181.
- [13] MARSZALEK P. E. *et al.*, *Nature (London)*, **402** (1999) 100.
- [14] HALPERIN A. and ZHULINA E. B., *Europhys. Lett.*, **15** (1991) 417.
- [15] GEISER P. E. and SHAKHNOVICH E. I., *Phys. Rev. E*, **65** (2002) 0506110.
- [16] GEISER P. E. and SHAKHNOVICH E. I., *Macromolecules*, **35** (2002) 4429.
- [17] FARAGO O., KANTOR Y. and KARDAR M., *Europhys. Lett.*, **60** (2002) 53.
- [18] MARENDUZZO D., MARITAN A., ROSA A. and SENO F., *Phys. Rev. Lett.*, **90** (2003) 088301.
- [19] ALLEN M. P. and TILDESLEY D. J., *Computer Simulations of Liquids* (Oxford University Press, London) 2001.
- [20] DI TOLLA F. D. and RONCHETTI M., *Phys. Rev. E*, **48** (1993) 1726.
- [21] LANDAU L. D. and LIFSHITZ E. M., *Fluid Mechanics* (Pergamon Press) 1959.
- [22] DOERING C. R., *Physica A*, **188** (1992) 386.
- [23] BEN-AVRAHAM D., *Phys. Rev. Lett.*, **81** (1998) 4756.
- [24] SPOUGE J. L., *Phys. Rev. Lett.*, **60** (1988) 871; *J. Phys. A*, **21** (1988) 4183.